Novel super-structures resulting from the coordination of chiral oxazolines on platinum nanoparticles

Montserrat Gómez,*[a] Karine Philippot,*[b] Vincent Collière,[b] Pierre Lecante,[c] Guillermo Muller[a] and Bruno Chaudret*[b]

[a] *Departament de Química Inorgànica, Universitat de Barcelona, Martí i Franquès 1-11, 08028 Barcelona, Spain. E-mail: montserrat.gomez@qi.ub.es*
[b] *Laboratoire de Chimie de Coordination du CNRS, 205, route de Narbonne, 31077 Toulouse Cedex 04, France. E-mail: phil@lcc-toulouse.fr, chaudret@lcc-toulouse.fr*
[c] *Centre d'Elaboration des Matériaux et d'Etudes Structurales du CNRS, 29, rue Jeanne Marvig, BP 4347, 31055 Toulouse Cedex, France*

Received (in Montpellier, France) 8th July 2002, Accepted 29th August 2002
First published as an Advance Article on the web 10th December 2002

The reaction of $Pt_2(dba)_3$ with CO in toluene leads rapidly to the formation of platinum nanoparticles which can be further stabilized by addition of aminoalcohol or oxazoline ligands. The coordination of the oxazoline ligands at the surface of the particles is demonstrated by IR after purification of the colloids. The fcc structure of the particles is evidenced by WAXS investigations, a statistical method which also gives information about the degree of crystallinity of the particles. TEM and HREM micrographs reveal surprising organisations of the particles into super-structures depending on the nature and/or position of the substituents present on the ligands. In addition, these particles are catalytically active in the hydrogenation of ethyl pyruvate, even if the preliminary results are modest.

Introduction

Metal nanoparticles appear more and more as novel chemical objects[1] with a high potential in terms of applications taking advantage of their unique properties in fields as diverse as catalysis,[2] micro-, nanoelectronics,[3] magnetism,[4] semi-conduction and optics.[5] In all these fields, it appears that the properties, both chemical and physical, require identical objects of a controlled size in order to be analysed, understood and further applied. Thus, it is clear that most of the properties related to nanoparticles are size and, in some cases, shape dependent (optics, magnetism).[6] The control of size and shape of the particles is therefore of primary importance. In addition, it has been stated that reproducibility has always been a problem when considering metal colloid synthesis.[7] It is obvious that any application requires that this problem be solved. We have developed in the past few years new general methods for the synthesis of metal particles of controlled size through an organometallic approach.[8] Perhaps the most important advantage of this approach is the possibility of accessing reproducibly clean surfaces which in a second step may be covered with stabilizing ligands.[8c,k] Such particles may also be reacted in an organized medium to give them an anisotropic shape.[9] Once these particles are formed, two parallel questions arise:

(i) If these particles are to have a future in chemistry, is it possible to tune their reactivity and selectivity in a way similar to that achieved in organometallic chemistry with mononuclear species? This will need development of the surface chemistry of the particles and of the ligands necessary for this purpose.

(ii) If these particles are to be employed for physical applications, how can they be addressed? The first and most studied answer to this question is to promote their self-organization through an organized medium or long chain ligands acting as surfactants. This approach has allowed the formation of crystalline arrays of self-assembled particles in 2 or 3 dimensions. Another answer can be, in a similar way to (i), to develop ligands adapted to the particles and able to interconnect through, for example, hydrogen bond networks. This approach has been extensively studied in coordination chemistry (molecular tectonics)[10] and recently extended to platinum nanoparticles *via* bifunctional thiolato ligands.[8j]

In both cases, it appears necessary to develop coordination chemistry at the surface of the nanoparticles and to find adapted ligands. Asymmetric ligands appear particularly appealing since they can induce an interesting catalytic activity and since, in the case of asymmetric induction, this would help to understand the coordination of ligands on the particle surface.[11] Furthermore, asymmetric ligands may promote the formation of anisotropic networks of hydrogen bonds. We have been interested in nitrogen based ligands such as chiral mono- and bis-oxazolines.[12] These ligands are easily prepared from β-aminoalcohols and nitrile or carboxylic acid derivatives[13] and display a widely studied chemistry[14] because of their potential applications to different enantioselective homogenous catalytic processes.[15] They have recently been tested as ligands for ruthenium nanoparticles used for catalytic hydrogenation reactions.[12] An aminoalcohol, namely 2-aminobutanol, which is a very simple asymmetric ligand, was also studied.

We report in this paper the synthesis of platinum nanoparticles stabilized by chiral ligands bearing various functional groups and the formation of super-structures induced by the ligands.

Results and discussion

We have previously reported the synthesis of platinum nanoparticles through reaction of CO with $Pt_2(dba)_3$ in THF or toluene and the addition of a variety of ligands such as CO,

 DOI: 10.1039/b206660m

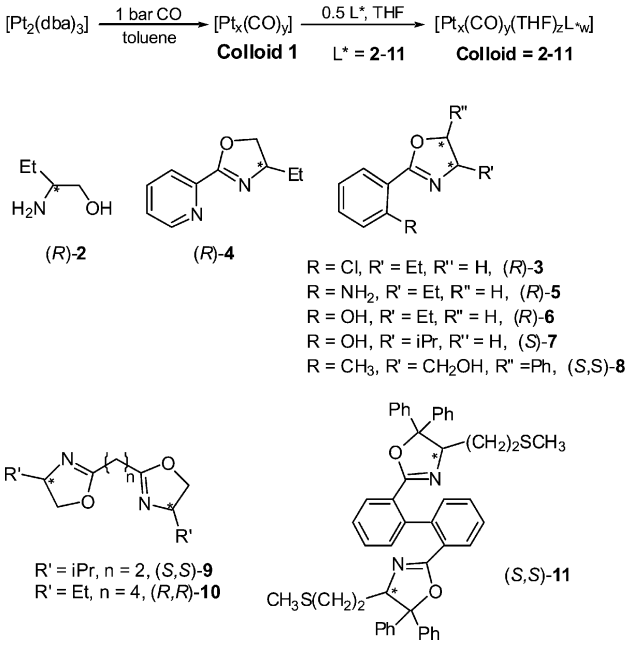

Scheme 1 Colloids synthesis with ligand structures.

THF, PPh_3 ,[8a] octanethiol[8c] and bifunctional thiolate ligands.[8j] A similar procedure was carried out, namely reaction of $Pt_2(dba)_3$ with 1 bar CO in toluene followed by addition of 0.5 equiv. of an asymmetric ligand in THF solution (Scheme 1). In each case, stable colloids, namely **Colloids 2–11**, were produced (Table 1). The particles could be isolated by evaporation to dryness and successive washings with pentane to produce dark brown to black powders. These powders could be redissolved in THF without decomposition. The particles display a diameter of *ca.* 1.5 nm and adopt the fcc structure of bulk platinum as evidenced by WAXS (Wide Angle X-ray Scattering) and HRTEM (High Resolution Transmission Electron Microscopy) studies. Infrared spectra show that the particles have kept CO ligands at their surface. The CO stretch observed for **Colloids 2–11** (in THF; 2045–2054 cm^{-1}) suggests little electronic influence of the ligands on the electron density of the particles. A more important effect has previously been found when using thiol ligands. νCO for $Pt_x(CO)_y(THF)_z$ and $Pt_x(CO)_y(THF)_z(octanethiol)_w$ colloids in THF are, respectively, 2052 and 2040 cm^{-1}, namely a shift of 12 cm^{-1} towards low frequency.[8c] This is not surprising given that oxazolines contain nitrogen and oxygen donor groups; this behaviour has also been previously observed when simple amines were used as stabilizers.[16] The CN stretch does not seem much affected by the coordination of the oxazoline on the platinum surface (see Table 1).

TEM and HRTEM studies show that in every case, in contrast to ruthenium nanoparticles of slightly larger size but stabilized by the same ligands,[12] the particles are not isolated but gather into super-structures. High resolution images, typical examples of which are shown in Figs. 1 and 2, demonstrate that the individual particles have kept their integrity, namely original size and structure, inside the super-structures. This therefore demonstrates that the super-structures result from the supramolecular assembly of the nanoclusters composed of one particle and the corresponding ligand shell, probably *via* the interaction of the surface ligands through hydrogen bonding. The morphologies of these super-structures are diverse, in some cases elegant and/or very surprising. They depend upon the nature and/or the position of the functional groups present on the ligands.

One of the most common super-structures is a disk which includes monodisperse particles regularly separated by 1 nm or less. This suggests the presence of an isotropic arrangement of the ligands around the platinum nanoparticles and the presence of a statistical hydrogen bond network. Such structures have been observed for **Colloids 3**, **4**, **5**, **8** and **11** (Figs. 3 and 4). In these cases, the bidentate ligands firmly coordinate to the surface of the particles and contain a bulky apolar lipophilic environment. The disk shape presumably results from an isotropic arrangement in solution building spheres which upon deposition onto the microscopy grid give this "disk" appearance. The weak interaction observed between nanoparticles may result from Van der Waals contacts between large lipophilic entities, or alternatively but less likely from the presence of traces of water which interconnect the oxygen atoms of the oxazoline ligands.

The second common super-structure adopts curious shapes which can be likened to dendrites, arborescences, sea-anemons (see Figs. 1, 5–8). The wires are generally connected at one extremity of the super-structure and are widely spread at the other extremity giving rise in many cases to monolayers. These wires are constituted of linearly connected particles, which means that the diameter of a typical nanowire is that of one nanoparticle (*ca.* 1.5 nm). This suggests strong hydrogen bonding in one direction and weak interactions between the nanowires. The ligands which generate this type of assembly (**L*2**, **5**, **7**, **9** and **10**; see Scheme 1) are typically bidentate ligands containing multiple polar groups able to give rise to hydrogen bonding. The most beautiful wires and arborescences are observed for ligands which can be associated through strong hydrogen bonds, typically "O–H···O", "O–H···N" or "N–H···N" (**Colloids 2**, **5**, **6** and **7**). This suggests the presence of both strong coordination of the ligands at the surface of the particles and of a second "coordination sphere" involving

Table 1 Data on new platinum colloids: ligand, CO and CN stretches, type of association observed by TEM and approximate particle mean size, structure

Colloids	Ligand L*	IR (KBr) νC=N in free ligand/cm^{-1}	IR (THF) νCO,νC=N in colloid/cm^{-1}	IR (KBr) νCO,νC=N in colloid/cm^{-1}	TEM type of association and approximate mean size	WAXS structure coherence length/nm
Colloid 2	(*R*)-2	—	2054	2031	dendrites #1.6–1.8 nm	—
Colloid 3	(*R*)-3	1653	2045, 1653	—	disks and nanowires and bundles *ca.* 1.5 nm	—
Colloid 4	(*R*)-4	1642	2045, 1642	2025, 1651	disks *ca.* 1.5 nm	—
Colloid 5	(*R*)-5	1636	2047, 1636	2034, 1633	disks and dendrites #1.2–1.3 nm	fcc #1.2–1.4
Colloid 6	(*R*)-6	1641	2051, 1643	2044, 1617	nanotubes *ca.* 1.2 nm	—
Colloid 7	(*S*)-7	1640	2052, 1644	2044, 1617	dendrites and nanocrystals #1.8 nm	fcc #1.8
Colloid 8	(*S*,*S*)-8	1636	2052, 1642	2042, 1633	monolayers and disks #1.2 nm	fcc #1.2
Colloid 9	(*S*,*S*)-9	1648	2047, 1672	2037, 1650	monolayers and dendrites #1.2 nm	fcc #1.2
Colloid 10	(*R*,*R*)-10	1651	2050, 1604	—	dendrites #1.5–1.8 nm	fcc #1.5–1.8
Colloid 11	(*S*,*S*)-11	1640	2047, 1654	2033, 1641	disks *ca.* 1.5 nm	—

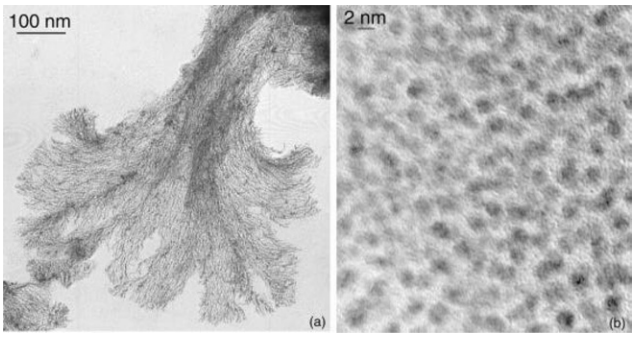

Fig. 1 TEM (a) and HRTEM (b) micrographs showing, respectively, the ''neuronal'' super-structures and atomic plans of the nanoparticles observed for **Colloid 2**.

ligands able to build strong hydrogen bond interactions between particles (see Scheme 2). The monodimensional character of these interactions is at first sight striking. It results most probably from the need to combine the polar regions where hydrogen bondings are present and the apolar ones which could be at the periphery of the wires. The presence of lipophilic regions at the periphery of the strong hydrogen bonds can explain the weak interactions observed between the nanowires.

In this respect, it is interesting to compare the results obtained with ligands **6** and **7**. These ligands are both constituted of a phenol group substituted in the *ortho* position by an oxazoline moiety. Furthermore, the oxazoline bears either an ethyl substituent (**L*6**) or an isopropyl one (**L*7**). In the case of **L*7**, in addition to the dendrites, very large rectangular super-structures of crystalline aspect are present; they account for most of the objects observed on the microscopy grid (Fig. 6). The simple substitution of the pendant isopropyl group by an ethyl one has a major effect on the assembly of the nanoparticles. This gives rise to very curious super-structures which at first sight resemble snakes displaying spots (Fig. 2). The high resolution image shows individual nanoparticles of 1.5 nm, *i.e.* of standard size, severely agglomerated. It is therefore possible that the ethyl substituent allows the formation of an isotropic hydrogen bond network which explain the presence of the small spheres (spots). The orientation of the snake body is more difficult to understand. In the case of **L*7**, the presence of the unidirectionality discussed above may explain the formation of the rectangular structures. Somewhat similar organisation into tubes has been previously observed when using *p*-hydroxy- and *p*-amino-thiophenol as stabilizers of similar platinum particles.[8j]

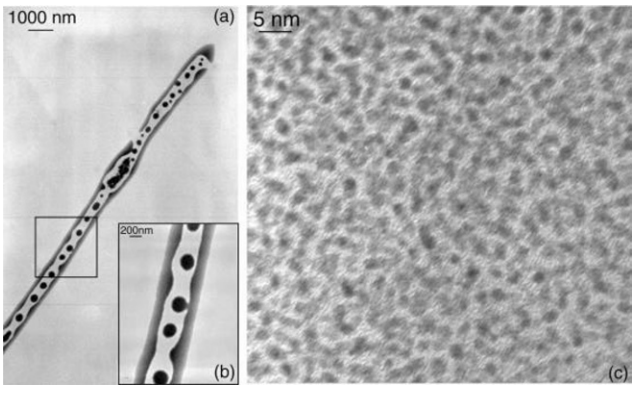

Fig. 2 TEM micrographs (a) and (b) at 2 different magnifications (5 and 20 K, respectively) and HRTEM micrograph (c) showing the nanotubes and their individual constitutive nanoparticles obtained for **Colloid 6**.

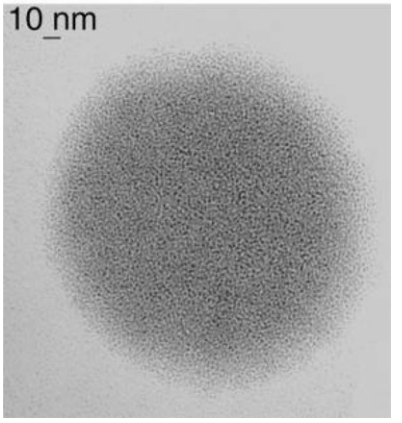

Fig. 3 TEM micrograph of disks resulting from the preparation of **Colloid 4**.

The case of the two bidentate bis-oxazoline ligands is also interesting. As stated above, both give rise to ''neuronal'' structures. However, whereas **L*9** shows standard individual particles linearly connected, a high resolution image of **Colloid 10** (Fig. 8) shows the presence in some areas of large coalesced particles displaying a high aspect ratio. This may be due to the presence of some mono N-coordinated bis-oxazoline (**L*10**) which could favour nanoparticle interconnexion and then coalescence. This process would be less probable in the case of **L*9** which contains only two carbon atom linkers.

Finally, the use of the chloro substituted ligand **3** as stabilizer leads to the formation of long and aligned nanowires (Fig. 9). The reason for this observation is not known. One hypothesis could be the activation of C–Cl bonds by platinum generating charges on the particles. Formation of ionic associations of surfactants (for example amine–carboxylic acid) have recently been found to be excellent for either the formation of monodisperse assemblies of nanoparticles or for controlling their aspect ratio.[6]

WAXS investigations on **Colloids 2**, **5**, **7** and **8** (Fig. 10) revealed in each case a pattern consistent with a fcc structure. The metal–metal distance is similar to that of bulk platinumin in agreement with the metallic nature of the particles but reduced by *ca.* 1% in all but one of the samples. In the case of **Colloid 7**, the reduction of the metal–ligand distance is more important (1.6%). These observations match previous ones[17] and suggest the presence at the surface of the particles of ligands not giving rise to strong metal–metal bonds. This is corroborated by an extended coherence length which matches the size deduced from TEM observations in the case of **Colloid 7**.

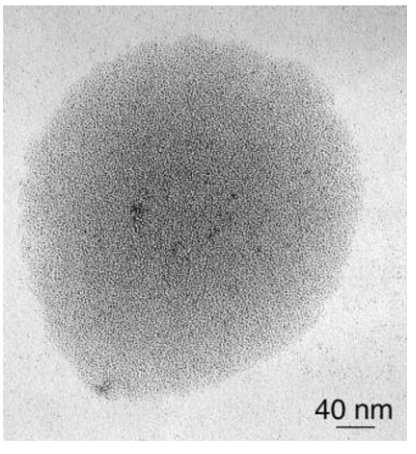

Fig. 4 TEM micrograph of **Colloid 8** showing nanoclusters organized in disks.

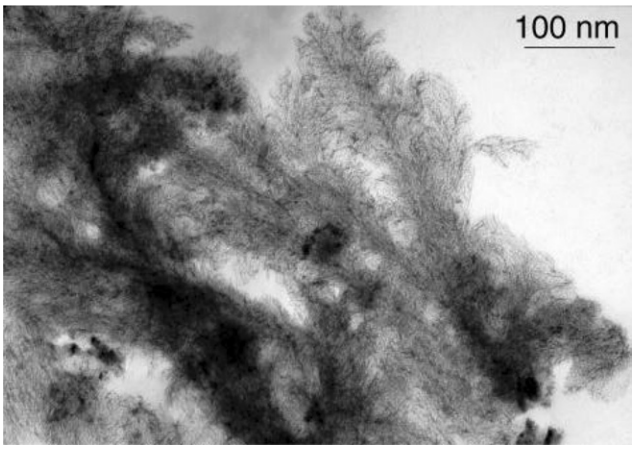

Fig. 5 TEM micrograph of **Colloid 5** evidencing the abundant formation of dendrites.

In the other cases, the peaks become broader and broader when considering successively **Colloids 2**, **5** and **8**. This may be indicative of a decrease in the degree of crystallinity, although we must be careful in the interpretation of such data. For **Colloids 9** and **10** (Fig. 11), the strong decrease in intensity observed for the first peaks suggests a variation of the metal–metal distance between the core and the surface of the particles and therefore a strong coordination of the surface ligands. Such behaviour has previously been noticed for octanethiol stabilized platinum particles. Indeed, in this case, a coherence length of 1.2 nm had been measured while a mean size of 1.6 nm was revealed by TEM. This discordance had been explained by a strong coordination of octanethiol ligands.[8c] Such good donor ligands would modify the metal–metal distances and the arrangement of the surface atoms in a way similar to molecular clusters. This had been confirmed by HRTEM investigations, showing for the octanethiol protected platinum particles a good crystallinity only in their core. A similar, albeit less pronounced, effect may be due in the present case to the chelate effect of the bis-oxazoline ligands.

The infrared spectra of all colloids were measured both in the solid state (KBr) and in solution (THF). In both cases, it is clear that the most important shift in the νCO frequency is observed when using ligands **3**, **4**, **5**, **9** and **11** which for various reasons have the best coordination ability (presence of, respectively, pyridine, amino or thioether groups, chelate effect). This has also been previously observed upon coordinating thiols at the surface of platinum particles.

As a further characterization of the coordination of the chiral ligands described hereabove, we investigated their reactivity for catalytic ethyl pyruvate hydrogenation. We found however in each case a low activity without asymmetric induction. This can result from the fluxionality of the oxazoline ligands at the surface of the particles. The presence of CO ligands at the surface of the particles may also be detrimental as they can act as a catalytic poison. Further work is presently in progress to avoid the presence of CO at the surface of the particles and then to obtain better catalysts.

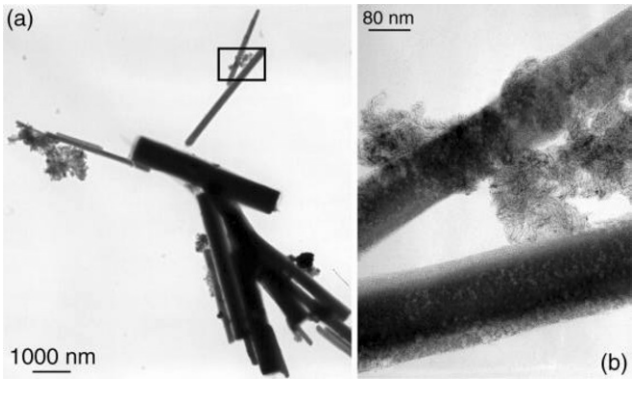

Fig. 6 TEM micrograph of **Colloid 7** showing nanocrystals (a) and an enlargement of a 2 nanocrystal junction (b).

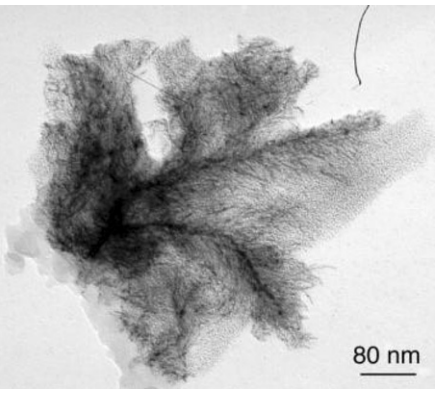

Fig. 7 TEM micrograph of dendrites corresponding to the **Colloid 9** assemblies.

Conclusion

This study demonstrates first that chiral polydentate ligands such as the oxazoline derivatives described here, efficiently stabilize very small platinum nanoparticles. A chelate effect is clearly demonstrated which leads to a better stabilization of the particles. The most interesting aspect of this work concerns the super-structures which can be generated by appropriate modulation of the ligands. Some of the ligands will firmly coordinate through polar bonds to the surface of platinum and leave an exposed lipophilic environment. This will give rise to weak interactions between the particles and formation of "spheres" or "disks" (**Colloids 4**, **8**, **11**). Another class of ligands, containing smaller organic substituents will allow the formation of hydrogen bond networks in given directions. This will result in the formation of nanowires which display a mean diameter corresponding to one nanoparticle and which assemble into sometimes spectacular super-structures (for example **Colloids 2**, **3**, **5**). Finally, in the case of small, polar and multifunctional ligands, 3D structures are observed (**Colloids 6** and **7**). Interestingly, in the latter case, some privileged orientations are still present which we do not explain.

It is thus possible with simple ligand engineering to orientate the connexion between particles and to adjust the inter-particle distance. This kind of approach towards the supramolecular arrangement of nanoparticles is only at the beginning but may prove fruitful for exploiting the physical properties of such nano-objects. In contrast, the catalytic properties of

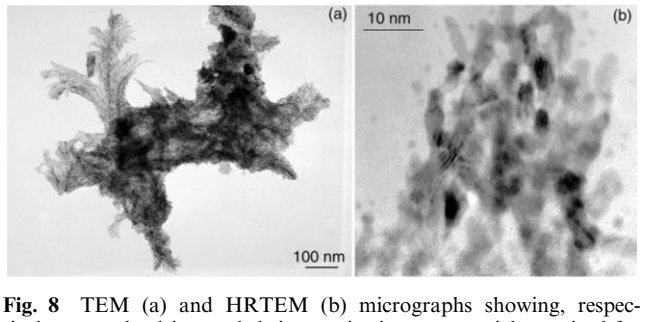

Fig. 8 TEM (a) and HRTEM (b) micrographs showing, respectively, some dendrites and their constitutive nanoparticles noticed for **Colloid 10**.

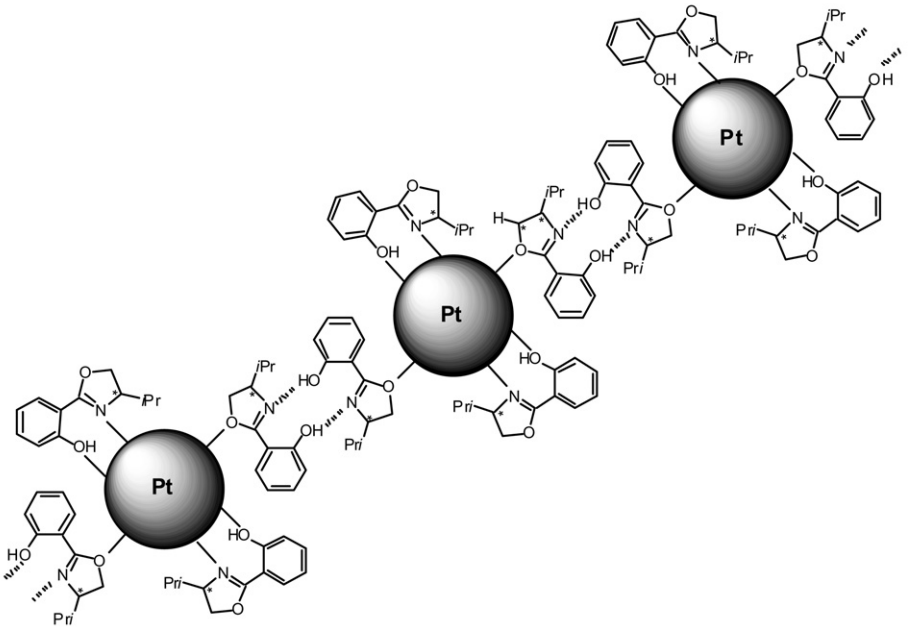

Scheme 2 Illustration of possible interactions between particles through strong hydrogen bonds between ligands in the case of **Colloid 7**.

these particles appeared disappointing but more relevant systems will be studied in the future.

Experimental section

General

All operations were carried out using standard Schlenk tube or Fischer–Porter bottle techniques or in a glove-box under argon. Solvents were purified just before use by distillation under a nitrogen atmosphere: toluene and THF over sodium benzophenone, pentane over calcium hydride. All the reactions have been monitored by IR spectroscopy.

Infrared spectra were recorded on a Perkin-Elmer IRFT GX 2000 spectrophotometer as colloidal solutions transferred into a KBr cell or using KBr pellets after isolation of the products as solids. The reference spectrum of the solvent was systematically subtracted.

The oxazoline-stabilized colloidal solutions were all prepared following the typical experiment described hereafter.

Materials

$Pt_2(dba)_3$ was prepared according to literature procedures.[18] Dba was purchased from Aldrich, (*R*)-2-aminobutanol from Fluka, K_2PtCl_4 from Johnson Matthey, CO from Air Liquid; all were used without purification. The oxazoline ligands were synthesized in the laboratory following a procedure previously published.[19]

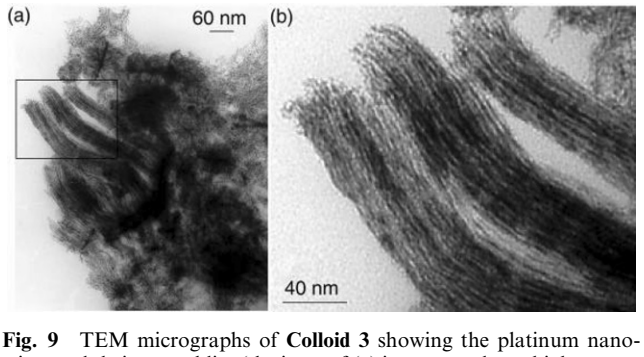

Fig. 9 TEM micrographs of **Colloid 3** showing the platinum nanowires and their assemblies (the inset of (a) is presented at a higher magnification in (b)).

TEM experiments

Specimens for TEM and HRTEM analysis were prepared, in a glove box, by slow evaporation of a drop of each crude colloidal solution deposited onto a holey carbon covered copper grid. The TEM experiments were performed at the "Service Commun de Microscopie Electronique de l'Université Paul Sabatier" on a JEOL 200 CX-T electron microscope operating at 200 kV with a point resolution of 4.5 Å. HRTEM observations were carried out with a JEOL JEM 2010 electron microscope working at 200 kV with a resolution point of 2.5 Å. The approximation of the particle mean size was made through a manual analysis of enlarged micrographs by measuring a number of particles on a given grid. Size distributions could not be obtained because of the small size of the particles and their inclusion into super-structures which resulted in some difficulty in distinguishing their limits.

WAXS experiments

All samples were sealed in Lindemann glass capillaries. Measurements of the X-ray intensity scattered by the sample

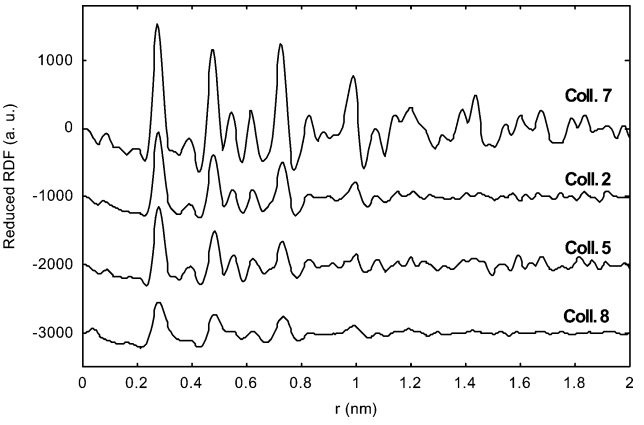

Fig. 10 RDF of particles of **Colloids 2**, **5**, **7** and **8**.

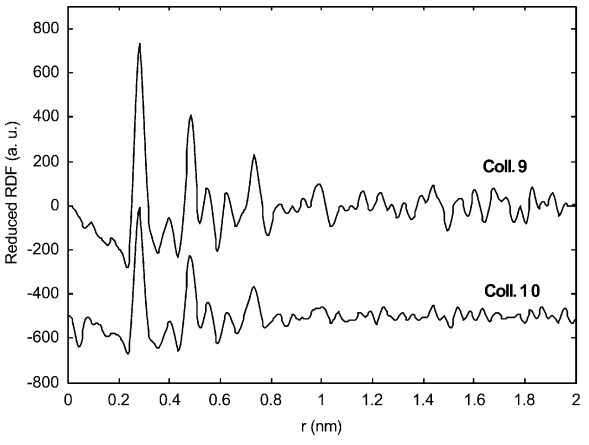

Fig. 11 RDF of particles of **Colloids 9** and **10**.

irradiated with graphite-monochromatized molybdenum K_α (0.071069 nm) radiation were performed using a dedicated two-axis diffractometer. In order to correct for the fluorescence from platinum, two scans were performed for each sample, one with an aluminium filter between the sample and the detector and another without filter. This procedure allowed for the accurate measurement of a fluorescence background. Time for data collection was typically 20 hours for a set of 457 values collected at room temperature in the range $0° < \theta < 65°$ for equidistant s values ($s = 4\pi(\sin\theta/\lambda)$; $\Delta s = 0.35$ nm^{-1}). In order to separate the intensity related to the particles from other contributions, scattering patterns from capillaries filled with pure ligands were also collected in the same conditions. The raw intensity was then corrected for the ligand scattering attenuated by sample absorption. Polarization and self-absorption corrections were also applied. Data were reduced using previously described procedures[20] in order to extract the structure-related component of WAXS, the so-called reduced intensity function(s), then Fourier transformed to allow for radial distribution function (RDF) analysis.

Compounds

Colloids 2–11 were prepared from the platinum precursor $Pt_2(dba)_3$ following a 2-steps procedure inspired of a previously described one;[8c] the chiral ligand was added subsequently to obtain **Colloid 2–11** as it is reported below.

In a first step, a solution of $Pt_2(dba)_3$ (100 mg, 0.091 mmol) in 40 ml of freshly distilled and degassed toluene in a Fischer-porter Bottle was pressurized with 1 bar of CO during 20 min under vigorous stirring. During this time the solution changed from deep purple to brown and a reddish-brown solid precipitated. The solution was removed by filtration and the precipitate was washed with pentane (4×20 ml) until the solution turned colorless, to eliminate dba, and dried under vacuum, giving then rise to **Colloid 1**. **IR Colloid 1** (KBr, cm^{-1}): 2052, 1811.

In a second step, a THF solution of the chosen chiral ligand (10 ml THF; 0.5 eq./Pt) was added to **Colloid 1** involving its redissolution and the obtention of a dark-brown colloidal solution. The mixture was left under vigorous stirring in solution for 12 hours at room temperature leading to **Colloid 2–11**. After that time, a small quantity of a black precipitate or sediment on walls of the schlenk tube was generally observed. Infrared spectra were recorded during this period of time (THF solutions), and also after isolation and purification of the colloids (KBr pellets). The CO and C=N stretches are given in Table 1. TEM and HRTEM analyses were performed after deposition of a drop of colloidal solutions onto holey carbon covered copper grids. The mean sizes, in a range 1.2 nm–1.8 nm, were estimate through a manual analysis of enlarged micrographs by measuring a number of particles on a given grid. After evaporation to dryness, the **Colloid 2–11** were isolated as dark brown powders and some of them could be analyzed by microanalysis: **Colloid 2**: %Pt = 70.42, %C = 20.50, %H = 2.20, %N = 4.82; **Colloid 4**: %C = 14.59, %H = 1.04, %N = 1.13; **Colloid 5**: %Pt = 61.33, %C = 26.65, %H = 2.38, %N = 3.20; **Colloid 7**: %C = 12.92, %H = 0.91, %N = 0.38; **Colloid 8**: %C = 38.16, %H = 2.82, %N = 1.96; **Colloid 9**: %Pt = 70.60, %C = 23.69, %H = 2.40, %N = 1.68; **Colloid 10**: %Pt = 45.76; **Colloid 11**: %Pt = 21.45, %C = 50.09, %H = 3.57, %N = 2.31. WAXS (Wide Angle X-Ray scattering) experiments were performed on **Colloid 5**, and **Colloids 7–10** evidencing the fcc structure of particles similar to that of the bulk platinum.

Acknowledgements

The authors thank Lucien Datas, TEMSCAN for TEM and HRTEM analyses, the CNRS, the Ministerio de la Ciencia y Tecnología (BQU2001-3358 and HF2001-0024) and the Departament d'Universitats, Recerca i Societat de la Informacio de la Generalitat de Catalunya for financial support. M.G. thanks the Ministerio de Educación Cultura y Deporte (PR2000-0178 0077107784) for a grant.

References

1 (*a*) G. Schmid, *Chem. Rev.*, 1992, **92**, 1709; (*b*) *Clusters and colloids, from theory to applications*, ed. G. Schmid, V.C.H., Weinheim, 1994; (*c*) *Nanotechnology, Molecularly Designed Materials*, ed. G.-M. Chow and K. E. Gonsalves, A.C.S. Symposium Series 622: Science and Engineering, Inc., 20–24 August 1995, American Chemical Society, Washington, DC, 1996; (*d*) K. J. Klabunde, G. Cardenas-Trivino, in *Active Metals: Preparation, Characterization, Applications*, ed. A. Fürstner, VCH, Weinheim, 1996, pp. 237–277; (*e*) N. Toshima and T. Yonezawa, *New J. Chem.*, 1998, 1179; (*f*) G. Schmid, M. Bäumle, M. Geerkens, I. Heim, C. Osemann and T. Sawitowski, *Chem. Soc. Rev.*, 1999, **28**, 179; (*g*) M. A. El-Sayed, *Acc. Chem. Res.*, 2001, **34**, 257.

2 (*a*) L. N. Lewis, *Chem. Rev.*, 1993, **93**, 2693; (*b*) L. N. Lewis, in *Catalysis by Di- and Polynuclear Metal Cluster Complexes*, ed. R. D. Adams and F. A. Cotton, Wiley-VCH Inc., New York, Weinheim, 1998, 373; (*c*) K. S. Weddle, J. D. Aiken III and R. G. Finke, *J. Am. Chem. Soc.*, 1998, **120**, 5653; (*d*) J. D. Aiken III and R. G. Finke, *J. Mol. Catal. A: Chem.*, 1999, **145**, 1; (*e*) H. Bönnemann, G. Braun, W. Brijoux, A. Schulze Tilling, K. Seevogel and K. Siepen, *J. Organomet. Chem.*, 1996, **520**, 143; (*f*) H. Bönnemann and G. A. Braun, *Chem. Eur. J.*, 1997, **3**, 1200; (*g*) J. U. Köhler and J. S. Bradley, *Langmuir*, 1998, **14**, 2730; (*h*) J. Schulz, A. Roucoux and H. Patin, *Chem. Eur. J.*, 2000, **6**, 618; (*i*) H. Bönnemann and R. M. Richards, *Eur. J. Inorg. Chem.*, 2001, 2455.

3 (*a*) M. Brust, D. Bethell, D. J. Schiffrin and C. J. Kiely, *Adv. Mater.*, 1995, **7**, 795; (*b*) M. D. Musick, C. D. Keating, M. H. Keefe and M. J. Natan, *Chem. Mater.*, 1997, **9**, 1499; (*c*) T. Oku and K. Suganuma, *Chem. Commun.*, 1999, 2355; (*d*) G. Schmid and N. Beyer, *Eur. J. Inorg. Chem.*, 2000, 835.

4 (*a*) L. G. de Jongh, *Physics and Chemistry of Metal Cluster Compounds*, Kluwer, Dordrecht, 1994; (*b*) K. A. Easom, K. J. Klabunde, C. M. Sorensen and G. C. Hadjipanayis, *Polyhedron*, 1994, **13**, 1197.

5 (*a*) L. M. Liz-Marzan and P. Mulvaney, *New J. Chem.*, 1998, 1285; (*b*) M. P. Pileni, *New J. Chem.*, 1998, **22**, 693.

6 See V. F. Puntes, K. M. Krishnan and A. P. Alivisatos, *Science*, 2001, **291**, 2115 and references therein.

7 J. S. Bradley in *Clusters and colloids, from theory to applications*, ed. G. Schmid, V.C.H., Weinheim, 1994, 459.

8 (*a*) A. Rodriguez, C. Amiens, B. Chaudret, M.-J. Casanove, P. Lecante and J. S. Bradley, *Chem. Mater.*, 1996, **8**, 1978; (*b*) M. Respaud, J.-M. Broto, H. Rakoto, A. R. Fert, L. Thomas, B. Barbara, M. Verelst, E. Snoeck, P. Lecante, A. Mosset, J. Osuna, T. Ould Ely, C. Amiens and B. Chaudret, *Phys. Rev. B*, 1998, **57**, 2925; (*c*) F. Dassenoy, K. Philippot, T. O. Ely, C. Amiens, P. Lecante, E. Snoeck, A. Mosset, M.-J. Casanove and B. Chaudret, *New J. Chem.*, 1998, **22**, 703; (*d*) T. Ould Ely,

C. Amiens, B. Chaudret, E. Snoeck, M. Verelst and M. Respaud, J.-M. Broto, *Chem. Mater.*, 1999, **11**, 526.(*e*) C. Pan, F. Dassenoy, M.-J. Casanove, K. Philippot, C. Amiens, P. Lecante, A. Mosset and B. Chaudret, *J. Phys. Chem. B*, 1999, **103**, 10 098; (*f*) C. Nayral, E. Viala, P. Fau, F. Senocq, J.-C. Jumas, A. Maisonnat and B. Chaudret, *Chem. Eur. J.*, 2000, **6**, 4082; (*g*) C. Nayral, E. Viala, V. Collière, P. Fau, F. Senocq, A. Maisonnat and B. Chaudret, *Appl. Surf. Sci.*, 2000, **164**, 219; (*h*) K. Soulantica, A. Maisonnat, M.-C. Fromen, M.-J. Casanove, P. Lecante and B. Chaudret, *Angew. Chem., Int. Ed.*, 2001, **40**, 448; (*i*) C. Pan, K. Pelzer, K. Philippot, B. Chaudret, F. Dassenoy, P. Lecante and M.-J. Casanove, *J. Am. Chem. Soc.*, 2001, **123**, 7584; (*j*) S. Gomez, L. Erades, K. Philippot, B. Chaudret, V. Collière, O. Balmes and J.-O. Bovin, *Chem. Commun.*, 2001, 1474.

9 N. Cordente, M. Respaud, F. Senocq, M.-J. Casanove, C. Amiens and B. Chaudret, *Nano Lett.*, 2001, **10**, 565.

10 M. V. Hosseini and A. de Cian, *Chem. Commun.*, 1998, 727.

11 (*a*) H. Bönnemann and G. A. Braun, *Chem. Eur.*, 1997, **3**, 1200; (*b*) J. U. Köhler and J. S. Bradley, *Langmuir*, 1998, **14**, 2730.

12 S. Jansat, K. Pelzer, K. Philippot, M. Gómez, B. Chaudret and G. Muller, unpublished data.

13 M. Reuman and A. I. Meyers, *Tetrahedron*, 1985, **41**, 837; M. Peer, J. C. de Jong, M. Kiefer, T. Langer, H. Rieck, H. Schell, P. Sennhenn, J. Sprinz, H. Steinhagen, B. Wiese and G. Helmchen, *Tetrahedron*, 1996, **52**, 7547.

14 M. Gómez, G. Muller and M. Rocamora, *Coord. Chem. Rev.*, 1999, **193–195**, 769.

15 (*a*) A. K. Ghosh, P. Mathivanan and J. Cappiello, *Tetrahedron: Asymmetry*, 1998, **9**, 1; (*b*) Y. Jiang, Q. Jiang and X. Zhang, *J. Am. Chem. Soc.*, 1998, **120**, 3817; (*c*) T. Langer and G. Helmchen, *Tetrahedron Lett.*, 1996, **37**, 1381; (*d*) Q. Jiang, D. van Plew, S. Murtuza and X. Zhang, *Tetrahedron Lett.*, 1996, **37**, 797; (*e*) R. Noyori and S. Hashiguchi, *Acc. Chem. Res.*, 1997, **30**, 97.

16 No published results.

17 F. Dassenoy, M.-J. Casanove, P. Lecante, C. Pan, K. Philippot, C. Amiens and B. Chaudret, *Phys. Rev. B*, 2001, **63**, 235407-3.

18 K. Moseley and P. M. Maitlis, *Chem. Commun.*, 1971, 982.

19 (*a*) M. Gómez, S. Jansat, G. Muller, M. A. Maestro and J. Mahía, *Organometallics*, 2002, **21**, 1077 and references therein; (*b*) M. Gómez, S. Jansat, G. Muller, D. Panyella, M. Font-Bardía and X. Solans, *J. Chem. Soc., Dalton Trans.*, 1997, 3755 and references therein.

20 M.-J. Casanove, P. Lecante, E. Snoeck, A. Mosset and C. Roucau, *J. Phys. III (France)*, 1997, **7**, 505.